NIH Public Access
Author Manuscript
J Magn Reson Imaging. Author manuscript; available in PMC 2014 August 01.

Published in final edited form as:
J Magn Reson Imaging. 2013 August ; 38(2): 454–459. doi:10.1002/jmri.23996.

Transmit B_1^+ Field Inhomogeneity and T_1 Estimation Errors in Breast DCE-MRI at 3T

Kyunghyun Sung, PhD[1,2,*], **Bruce L Daniel, MD**[1], and **Brian A Hargreaves, PhD**[1]
[1]Department of Radiology, Stanford University, Stanford, California, USA
[2]Department of Radiological Sciences, UCLA, Los Angeles, California, USA

Abstract

Purpose—To quantify B_1^+ variation across the breasts and to evaluate the accuracy of pre-contrast T_1 estimation with and without B_1^+ variation in breast MRI patients at 3T.

Materials and Methods—B_1^+ and variable flip angle (VFA) T_1 mapping were included in our dynamic contrast-enhanced (DCE) breast imaging protocol to study a total of 25 patients on a 3.0T GE MR 750 system. We computed pre-contrast T_1 relaxation in fat, which we assumed to be consistent across a cohort of breast imaging subjects, with and without compensation for B_1^+ variation. The mean and standard deviation of B_1^+ and T_1 values were calculated for statistical data analysis.

Results—Our measurements showed a consistent B_1^+ field difference between the left and right breasts. The left breast has an average 15.4% higher flip angle than the prescribed flip angle, and the right breast has an average 17.6% lower flip angle than the prescribed flip angle. This average 33% flip angle difference, which can be vendor and model specific, creates a 52% T_1 estimation bias in fat between breasts using the VFA T_1 mapping technique. The T_1 variation is reduced to 7% by including B_1^+ correction.

Conclusion—We have shown that severe B_1^+ variation over the breasts can cause a substantial error in T_1 estimation between the breasts, in VFA T_1 maps at 3T, but that compensating for these variations can considerably improve accuracy of T_1 measurements, which can directly benefit quantitative breast DCE-MRI at 3T.

Keywords

Breast imaging; Quantitative DCE-MRI; B_1 field inhomogeneity; T_1 mapping; High-field MRI

INTRODUCTION

Dynamic contrast-enhanced MRI (DCE-MRI) is a widely used method in the diagnosis of breast cancer (1,2). The technique typically acquires a time series of T_1-weighted images before and after injection of an intravenous low molecular-weight paramagnetic contrast agent, and can be used to characterize lesions of breast tissue. Quantitative microvascular properties can also be extracted by either fitting the gadolinium concentration curve to a pharmacokinetic model (3) or computing initial area under the gadolinium concentration curve (4). Both high spatial and high temporal resolution are important to accurately estimate these quantitative properties, which can potentially provide predictive, prognostic and pharmacodynamic response biomarkers for cancers (5-7).

[*]**Correspondence to:** Department of Radiological Sciences 300 UCLA Medical Plaza, Suite B119 Los Angeles, CA 90095 Phone: (310) 267-6842 Fax: (310) 825-9118 ksung@mednet.ucla.edu.

NIH-PA Author Manuscript
NIH-PA Author Manuscript
NIH-PA Author Manuscript

NIH-PA Author Manuscript

NIH-PA Author Manuscript

NIH-PA Author Manuscript

An image of pre-contrast T_1 values, registered to the dynamic series, is necessary to convert the dynamic MR data into the gadolinium concentration, where the concentration changes over time can be used to extract quantitative or semi-quantitative microvascular properties (8). One common method to measure T_1 is variable flip angle (VFA) imaging, also known as Driven Equilibrium Single-Pulse Observation of T1 (DESPOT1), which uses several short TR RF-spoiled gradient-echo (SPGR) acquisitions with varying flip angles (9-11). The VFA method is highly time efficient and allows rapid 3D volumetric T_1 mapping with high resolution (9,12), using the same pulse sequence that is used for the DCE acquisition itself, thus avoiding registration and calibration differences.

Non-uniformity of the transmit radio frequency (B_1^+) field can cause the actual flip angle in tissue to be different from the prescribed or nominal flip angle. The B_1^+ inhomogeneity tends to become more severe for higher field strengths, and at 3 Tesla, noticeable B_1^+ variation over the chest has been observed by many studies (13-16). The flip angle variation tends to be around 30 - 50% in the chest (13,14) and 40% across the breast (15,16), and can result in significant deviation in T_1 measurements using VFA (17,18). Therefore, careful consideration of the B_1^+ inhomogeneity will be important to achieve accurate T_1 mapping.

In this work, we measure B_1^+ inhomogeneity and pre-contrast T_1 values to test the accuracy of VFA T_1 mapping in the breast at 3T using the spatial consistency of T_1 estimates of fat, derived from fat-only 2-point Dixon VFA images, as a metric of improvement. We quantify the B_1^+ inhomogeneity in a total of 25 breast MRI patients at 3T and evaluate the accuracy of the T_1 measurements with and without compensation for B_1^+ variation by comparing T_1 relaxation times in fat between breasts as well as with a previously-reported value of the breast at 3T.

MATERIALS AND METHODS

Experiments were performed on a 3.0T GE MR 750 system (GE Healthcare, Waukesha, WI). A body coil was used for RF transmission and a commercially available 8-channel high-density breast array coil (GE Healthcare, Waukesha, WI) was used for signal reception. No parallel imaging was used. The automatic pre-scan, provided by the scanner, was used to calibrate the RF transmission gain, and the difference in nominal transmit gains between T_1 and B_1^+ measurements was applied to achieve a consistent flip angle variation between two sequences.

The B_1^+ measurement sequence and the T_1 VFA measurement sequence were performed as part of our standard clinical breast DCE-MRI protocol. Although other faster alternatives for B_1^+ mapping exist, we used a double angle method (DAM) to measure flip angle variation (19,20), as it is robust. We acquired both measurements in a total of 25 women undergoing clinically indicated breast MRI for a history of known or suspected breast disease, ranging in age between 26 and 73 years (age = 50.1 ± 11.4 years and mass = 62.4 ± 10.8 kg). The axial orientation was chosen for both measurements as it is commonly used in breast MRI, and a large B_1^+ variation is expected from left to right. This retrospective review and analysis of the B_1^+ and T_1 VFA data was performed in accordance with a protocol approved by our Institutional Review Board. More details on both measurement sequences are described below.

T_1 Measurements - Variable Flip Angle (VFA)

In VFA T_1 mapping, the measured signal intensity using SPGR (S_{SPGR}) can be used to compute a T_1 value in a linear form:

NIH-PA Author Manuscript

NIH-PA Author Manuscript

NIH-PA Author Manuscript

$$\frac{S_{SPGR}}{\sin\alpha} = E_1 \frac{S_{SPGR}}{\tan\alpha} + M_0 (1 - E_1) \quad [1]$$

where α is the flip angle, $E_1 = e^{-TR/T1}$ and M_0 is the longitudinal magnetization. By applying different flip angles α_n, we can generate different points ($S_{SPGR}/\sin\alpha_n$, $S_{SPGR}/\tan\alpha_n$) in the linearized form. The slope E_1 can then be estimated by linear regression, and T_1 can be extracted from E_1 using:

$$T_1 = \frac{TR}{\ln(E_1)} \quad [2]$$

Note that Eq. [[2] is highly sensitive to any possible errors on the linear regression. Any perturbation on flip angles α_n can degrade the slope estimation, and for example, +1% and −1% errors in the slope can range T_1 to be from 200 ms to 2000 ms, when the actual T_1 is 370 ms (TR = 4.5 ms).

T_1 maps were measured by using a 3D SPGR sequence with a dual-echo bipolar readout, where TEs were chosen to be in- and out-of-phase images (TE = 1.2/2.4 ms). A two-point Dixon fat-water separation algorithm was used to generate fat-only and water-only images (21), which can eliminate partial volume effects of the admixture of fat and glandular tissue in breasts (22). We placed the T_1 mapping before the pre-contrast T_1-weighted imaging and selected two flip angles to be 5° and 10°, which were optimized to symmetrically sample the signal curve of fat (T_1 was assumed to be 400 ms and TR = 4 ms in numerical simulation). We used T_1 measurements on the lipid component in fat and compared T_1 relaxation in fat with and without compensation for B_1^+ variation. Other imaging parameters were as follows: acquisition matrix size = 256×128×88, slice thickness = 4.2 mm, FOV = 32 cm, and total scan time = 20 sec.

B_1^+ Measurements - Double Angle Method (DAM)

B_1^+ maps were measured by using a 2D multi-slice SPGR sequence with prescribed flip angles of α and 2α (α = 60°). The actual flip angle map $\tilde{\alpha}$ was calculated as

$$\tilde{\alpha} = \arccos\left(\frac{I_{2\alpha}}{2I_\alpha}\right) \quad [3]$$

where I_α and $I_{2\alpha}$ are the magnitude images nominal flip angles of α and 2α. Note that any image non-uniformities except for the flip angle variation are cancelled out here as they are identical for both magnitude images. B_1^+ mapping followed the DCE-MRI acquisition, and repetition time (TR) of 5 seconds was used to ensure complete T_1 relaxation recovery of all tissue. Other imaging parameters were as follows: echo time (TE) = 2.5 ms, acquisition matrix = 64 × 64, number of slices = 49, slice thickness = 4 mm, field-of-view (FOV) = 44 cm, and total scan time = 9 min. Flip angle maps were computed using Eq. [3], and an error due to imperfect 2D slice profile was corrected by simulating the actual slice profile (23). We pre-computed a look-up table that corrects the slice profile errors based on the RF pulses (Hamming windowed sinc shape with different time-bandwidth products). An actual flip angle map can then be normalized by the prescribed flip angle (60°) to compute the relative flip angle variation in %.

Image Analysis

All image analysis both B_1^+ and T_1 maps was performed on OsiriX, an open source image visualization software application (24). OsiriX supports a complete plug-in architecture and shares all the advanced features with any plug-in developments. We have developed OsiriX

NIH-PA Author Manuscript

NIH-PA Author Manuscript

NIH-PA Author Manuscript

plug-ins to easily compute both B_1^+ and T_1 maps, shown in Fig. 1, and freely available at http://bmr.stanford.edu/. We aligned the orientation and resampled the relative flip angle variation to match the number of slices with the VFA images (using the "Resample" function in OsiriX). T_1 maps were computed using Eq. [2] with and without correcting B_1^+ variation. We only used central slices for comparison, to avoid effects from an imperfect 3D slab profile. We manually defined circular regions of interest (ROIs) covering medial and lateral portions of both left and right breasts based on magnitude fat-only images. We computed the mean and standard deviation (SD) across all 25 breast MRI patients and also drew box plots for data analysis (25).

RESULTS

Figure 2 shows an example of relative flip angle distribution in three orthogonal planes (axial, coronal and sagittal). One of the DAM images (I_{60}) is shown for the anatomical reference, and the coronal and sagittal planes are reformatted from 2D multi-slice images. In this subject, the left breast has an average 13% (± 4.3 %) higher flip angle than the prescribed flip angle, while the right breast has an average 20% (± 5 %) lower flip angle than the prescribed flip angle.

Figure 3a shows the mean and standard deviation of the relative flip angle variation across different slice locations (over a 11.5 cm range of axial slice locations) in a single subject. There exists a somewhat consistent flip angle difference between left and right breasts at all through-plane locations, and in this subject, the overall flip angle difference between the left and right breasts is approximately 35% (solid lines indicate the average relative flip angles of the left and right breasts). Figure 3b shows box plots (median, 25^{th} and 75^{th} percentiles, and lower and upper extremes) of the relative flip angle variation in all 25 breast MRI patients. The mean and standard deviation of the relative flip angle variation are 115.4 ± 9.3 (mean ± SD) % on the left breast and 82.4 ± 6.9% on the right breast, which conform to the literature (16).

Figure 4 shows pre-contrast T_1 values of fat with and without compensation for B_1^+ inhomogeneity in one subject. One of the fat only images (VFA, FA = 10°) and the relative flip angle map are displayed for the anatomical reference. The T_1 map generated using the prescribed flip angles of 5° and 10° has a substantial T_1 difference between the left and right breasts, while the B_1^+ compensated map shows more uniform fat T_1 across the whole breast. Average fat T_1 values over ROIs (see red dots in Fig 4) are 458 ms on the left ROI and 227 ms on the right ROI before B_1^+ correction, and become 387 ms on the left ROI and 323 ms on the right ROI after B_1^+ correction. The relative flip angle variation is 109% on the left ROI and 81% on the right ROI.

Figure 5 shows box plots (median, 25^{th} and 75^{th} percentiles, and lower and upper extremes) of T_1 estimation of fat with and without compensation for B_1^+ variation in all 25 breast MRI patients. The estimated T_1 values of fat without B_1^+ correction are 497.9 ± 112.1 ms on the left ROI and 239.0 ± 44.4 ms on the right ROI, while the estimated T_1 values of fat with B_1^+ correction are 374.4 ± 44.8 ms on the left ROI and 346.5 ± 35.1 ms on the right ROI. The T_1 difference between the left and right ROIs is 52% and is reduced to 7% after correcting for the B_1^+ variation. More importantly, the estimated fat T_1 values with B_1^+ correction are close to the literature-reported value (T_1 = 366 ms and solid gray lines in Fig 5) (22).

DISCUSSION

We have measured B_1^+ inhomogeneity over the breast in 25 breast MRI patients and have shown improved T_1 measurements by accounting for B_1^+ variation in 3T breast imaging.

NIH-PA Author Manuscript

NIH-PA Author Manuscript

NIH-PA Author Manuscript

Average relative flip angle variations were 115% (on the left breast) and 82% (on the right breast), where the overall difference between two breasts was approximately 35% and confirms to the literature (16). This flip angle difference mainly caused a 52% T_1 estimation bias, as measured in fat, between the left and right breasts, and we were able to reduce this estimation error to 7% by including B_1^+ correction.

We assumed the T_1 relaxation times in fat to be globally uniform and used the estimated fat T_1 fat as a reference to demonstrate a T_1 measurement bias. Corrected T_1 values in fat are 374 ms (on the left breast) and 347 ms (on the right breast), which are close to the literature-reported value, 366 ms (22). There still exists a small residual difference between two breasts, and we believe the residual bias can be further reduced by increasing the number of flip angles in the T_1 mapping (i.e., more than two flip angles).

Two flip angles in VFA T_1 mapping may not be enough to accurately measure T_1 due to its distinctive flip angle variation between two breasts at 3T. A set of flip angles can be optimized by accounting for the typical patterns of B_1^+ variation in the breast. The overall flip angle difference between the left and right breasts is relatively consistent among the patients, as shown in Fig 3, and we can design two different sets of flip angles (one for the left and the other for the right) by coarsely assuming the expected flip angle variation or can design a set of flip angles to make up for strong B_1^+ variations within one breast. We expect these approaches can be more useful for longer T_1 values such as fibroglandular tissue T_1, where the T_1 estimation is known to be more sensitive to the flip angle variation.

Multi-channel parallel excitation techniques can be used to reduce the bias in T_1 estimation due to B_1^+ inhomogeneity. A recent study has shown that dual-source excitation can improve B_1^+ inhomogeneity over conventional single-source excitation in breast MRI at 3T (26). This parallel excitation technique, however, requires special hardware equipment and can be vendor specific. In addition, the dual-source excitation can correct large first-order B_1^+ variations but can not solve all spatial variations, which may still cause a residual bias in T_1 estimation.

The effects of the T_1 estimation bias can also be minimized by pursuing other alternative quantification options. New enhancement indices that are insensitive to the variation of pre-contrast T_1 (T_{10}) values and B_1^+ inhomogeneity have been proposed to quantify the contrast agent uptake in DCE-MRI (27). The study has shown that these new enhancement indices, derived from saturation-recovery snapshot-FLASH (SRSF) images, are considerably less affected by errors caused by variations in the T_{10} and B_1^+ inhomogeneity at the cost of longer total scan time than the enhancement ratio in breast DCE-MRI.

Our study has several limiations. Although the degree of the flip angle variation agrees with the previous literature (15,16), the observed patterns of B_1^+ variation can be vendor and model specific as our study was performed on a 3T GE MR scanner. In addition, we have shown that our B_1^+ correction scheme can improve the accuracy of T_1 estimation, but this correction scheme can propagate noise to the T_1 estimation, which might make it less useful in low-SNR protocols. Other B_1^+ mapping methods (28-30) that are fast and can provide an improved angle-to-noise ratio can be considered to reduce the total scan time and error propagation.

In conclusion, we have shown that there exists a noticeable and somewhat systematic B_1^+ variation between the left and right breasts (average 33%) and have evaluated the accuracy of VFA T_1 mapping with and without compensation for B_1^+ variation at 3T. The average difference in fat T_1 between breasts was 52% in a total of 25 breast MRI patients, and we reduced this T_1 estimation error to 7% by accounting for B_1^+ variation, where the fat T_1

NIH-PA Author Manuscript

NIH-PA Author Manuscript

NIH-PA Author Manuscript

values are close to the literature-reported value. This improved T_1 measurement scheme can benefit quantitative breast DCE-MRI at 3T.

Acknowledgments

Grant Sponsors: NIH R01-EB009055

NIH P41-EB015891

GE Healthcare

REFERENCES

(1). Kuhl C. MRI of breast tumors. European radiology. 2000; 10:46–58. [PubMed: 10663717]

(2). Hayes C, Padhani A, Leach M. Assessing changes in tumour vascular function using dynamic contrast-enhanced magnetic resonance imaging. NMR in Biomedicine. 2002; 15:154–163. [PubMed: 11870911]

(3). Tofts PS, Brix G, Buckley DL, Evelhoch JL, Henderson E, Knopp MV, Larsson HBW, Lee TY, Mayr NA, Parker GJM. Estimating kinetic parameters from dynamic contrast-enhanced T1-Weighted MRI of a diffusable tracer: Standardized quantities and symbols. J. Magn. Reson. Imaging. 1999; 10:223–232. [PubMed: 10508281]

(4). Evelhoch JL. Key factors in the acquisition of contrast kinetic data for oncology. J. Magn. Reson. Imaging. 1999; 10:254–259. [PubMed: 10508284]

(5). Esserman L, Hylton N, Yassa L, Barclay J, Frankel S, Sickles E. Utility of magnetic resonance imaging in the management of breast cancer: evidence for improved preoperative staging. Journal of clinical oncology. 1999; 17:110–110. [PubMed: 10458224]

(6). Hawighorst H, Weikel W, Knapstein P, Knopp M, Zuna I, Schönberg S, Vaupel P, van Kaick G. Angiogenic activity of cervical carcinoma: assessment by functional magnetic resonance imaging-based parameters and a histomorphological approach in correlation with disease outcome. Clinical cancer research. 1998; 4:2305–2312. [PubMed: 9796959]

(7). Zahra M, Hollingsworth K, Sala E, Lomas D, Tan L. Dynamic contrast-enhanced MRI as a predictor of tumour response to radiotherapy. The Lancet Oncology. 2007; 8:63–74. [PubMed: 17196512]

(8). Larsson HBW, Stubgaard M, Frederiksen JL, Jensen M, Henriksen O, Paulson OB. Quantitation of blood-brain barrier defect by magnetic resonance imaging and gadolinium-DTPA in patients with multiple sclerosis and brain tumors. Magn. Reson. Med. 1990; 16:117–131. [PubMed: 2255233]

(9). Deoni SCL, Rutt BK, Peters TM. Rapid combined T1 and T2 mapping using gradient recalled acquisition in the steady state. Magn. Reson. Med. 2003; 49:515–526. [PubMed: 12594755]

(10). Brookes J, Redpath T, Gilbert F, Murray A, Staff R. Accuracy of T1 measurement in dynamic contrast-enhanced breast MRI using two-and three-dimensional variable flip angle fast low-angle shot. J. Magn. Reson. Imaging. 1999; 9:163–171. [PubMed: 10077009]

(11). Zhu X, Li K, KamalyAsl I, Checkley D, Tessier J, Waterton J, Jackson A. Quantification of endothelial permeability, leakage space, and blood volume in brain tumors using combined T1 and T2* contrast-enhanced dynamic MR imaging. J. Magn. Reson. Imaging. 2000; 11:575–585. [PubMed: 10862055]

(12). Wang H, Riederer S, Lee J. Optimizing the precision in T1 relaxation estimation using limited flip angles. Magn. Reson. Med. 1987; 5:399–416. [PubMed: 3431401]

(13). Greenman RL, Shirosky JE, Mulkern RV, Rofsky NM. Double inversion black-blood fast spin-echo imaging of the human heart: A comparison between 1.5T and 3.0T. J. Magn. Reson. Imaging. 2003; 17:648–655. [PubMed: 12766893]

(14). Sung K, Nayak KS. Measurement and characterization of RF nonuniformity over the heart at 3T using body coil transmission. J. Magn. Reson. Imaging. 2008; 27:643–648. [PubMed: 18306272]

(15). Kuhl CK, Kooijman H, Gieseke J, Schild HH. Effect of B1 inhomogeneity on breast MR imaging at 3.0 T. Radiology. 2007; 244:929–930. [PubMed: 17709843]

NIH-PA Author Manuscript

NIH-PA Author Manuscript

NIH-PA Author Manuscript

(16). Azlan CA, DiGiovanni P, Ahearn TS, Semple SIK, Gilbert FJ, Redpath TW. B1 transmission-field inhomogeneity and enhancement ratio errors in dynamic contrast-enhanced MRI (DCE-MRI) of the breast at 3T. J. Magn. Reson. Imaging. 2010; 31:234–239. [PubMed: 20027594]

(17). Treier R, Steingoetter A, Fried M, Schwizer W, Boesiger P. Optimized and combined T1 and B1 mapping technique for fast and accurate T1 quantification in contrast-enhanced abdominal MRI. Magn. Reson. Med. 2007; 57:568–576. [PubMed: 17326175]

(18). DiGiovanni P, Azlan C, Ahearn T, Semple S, Gilbert F, Redpath T. The accuracy of pharmacokinetic parameter measurement in DCE-MRI of the breast at 3 T. Physics in Medicine and Biology. 2010; 55:121. [PubMed: 20009182]

(19). Insko, EK.; Bolinger, L. B_1 mapping. Proc., SMRM, 11th Annual Meeting; Berlin. 1992. p. 4302

(20). Stollberger, R.; Wach, P.; McKinnon, G.; Justich, E.; Ebner, F. Rf-field mapping in vivo. Proc., SMRM, 7th Annual Meeting; San Francisco. 1988. p. 106

(21). Ma J. Breath-hold water and fat imaging using a dual-echo two-point dixon technique with an efficient and robust phase-correction algorithm. Magn. Reson. Med. 2004; 52:415–419. [PubMed: 15282827]

(22). Rakow-Penner R, Daniel B, Yu H, SawyerGlover A, Glover G. Relaxation times of breast tissue at 1.5 T and 3T measured using IDEAL. J. Magn. Reson. Imaging. 2006; 23:87–91. [PubMed: 16315211]

(23). Schär M, Vonken E, Stuber M. Simultaneous B0-and B1+-map acquisition for fast localized shim, frequency, and RF power determination in the heart at 3 T. Magn. Reson. Med. 2010; 63:419–426. [PubMed: 20099330]

(24). Rosset A, Spadola L, Ratib O. OsiriX: an open-source software for navigating in multidimensional DICOM images. J Digit Imaging. 2004; 17:205–216. [PubMed: 15534753]

(25). McGill R, Tukey JW, Larsen WA. Variations of box plots. American Statistician. 1978:12–16.

(26). Rahbar H, Partridge SC, DeMartini WB, Gutierrez RL, Parsian S, Lehman CD. Improved B1 homogeneity of 3 tesla breast MRI using dual-source parallel radiofrequency excitation. J. Magn. Reson. Imaging. 2012; 35:1222–1226. [PubMed: 22282269]

(27). Azlan CA, Ahearn TS, DiGiovanni P, Semple SIK, Gilbert FJ, Redpath TW. Quantification techniques to minimize the effects of native T1 variation and B1 inhomogeneity in dynamic contrast-enhanced MRI of the breast at 3 T. Magn. Reson. Med. 2011; 67:531–540. [PubMed: 21656561]

(28). Cunningham CH, Pauly JM, Nayak KS. SDAM: Saturated double angle method for rapid B1+ mapping. Magn. Reson. Med. 2006; 55:1326–1333. [PubMed: 16683260]

(29). Yarnykh V. Actual flip-angle imaging in the pulsed steady state: a method for rapid three-dimensional mapping of the transmitted radiofrequency field. Magn. Reson. Med. 2007; 57:192–200. [PubMed: 17191242]

(30). Sacolick L, Wiesinger F, Hancu I, Vogel M. B1 mapping by Bloch-Siegert shift. Magn. Reson. Med. 2010; 63:1315–1322. [PubMed: 20432302]

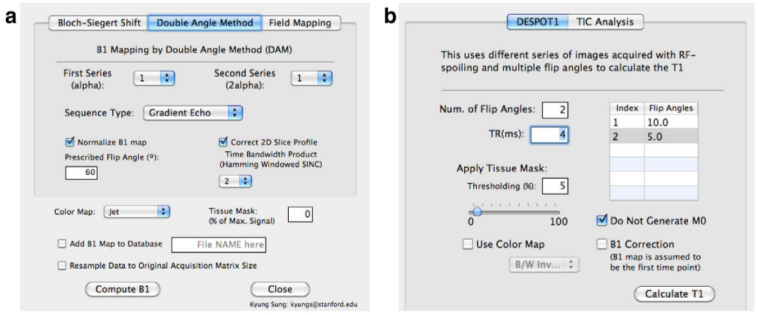

Figure 1.

Screenshots of OsiriX plug-ins for (a) B_1^+ measurements and (b) T_1 measurements. These plug-ins can allow easily computing all quantitative analysis and are freely available.

NIH-PA Author Manuscript NIH-PA Author Manuscript NIH-PA Author Manuscript

NIH-PA Author Manuscript

NIH-PA Author Manuscript

NIH-PA Author Manuscript

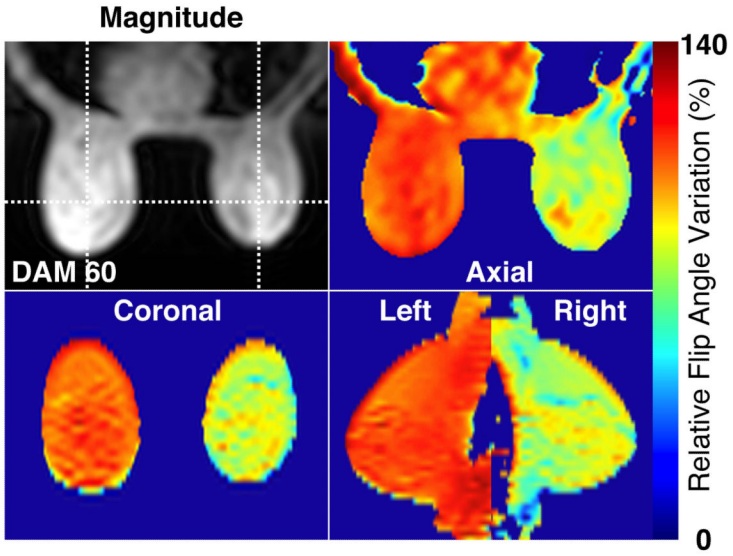

Figure 2.
An example of relative flip angle variation in percentage on a subject at 3T. One of the double angle method images is shown as an anatomical reference, and relative flip angle maps are shown in three orthogonal planes (axial, coronal, and sagittal).

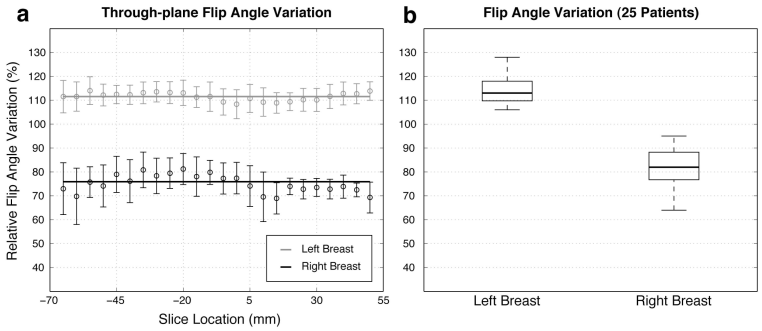

Figure 3.

(a) Relative flip angle variation across through-plane slices (−65 mm – 50 mm) for one patient. (b) Comparison of flip angle variation in the left and right breasts in 25 breast MRI patients using a box plot. The central mark on each box is the median, the edges of the box are the 25th and 75th percentiles, and the “whiskers” extend to the most extreme data points that were not considered outliers.

NIH-PA Author Manuscript
NIH-PA Author Manuscript
NIH-PA Author Manuscript

NIH-PA Author Manuscript

NIH-PA Author Manuscript

NIH-PA Author Manuscript

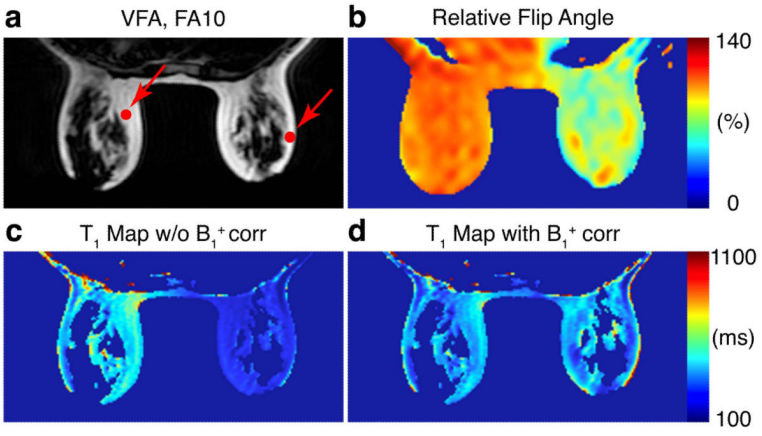

Figure 4.

(a) One of the VFA images and (b) relative flip angle map are shown as an anatomical reference. Comparison of T_1 estimation of fat (c) without and (d) with correcting B_1^+ inhomogeneity.

NIH-PA Author Manuscript

NIH-PA Author Manuscript

NIH-PA Author Manuscript

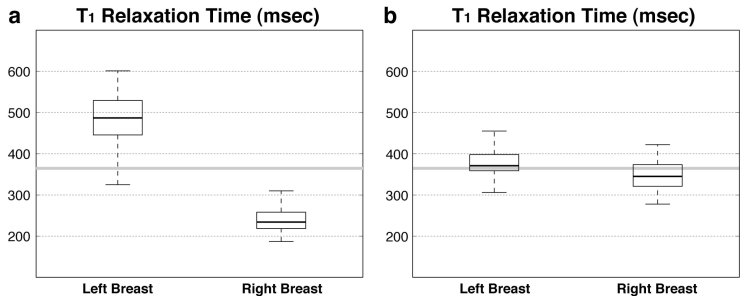

Figure 5.

Comparison of T_1 estimation in fat (a) without and (b) with correction of B_1^+ inhomogeneity in 25 breast MRI patients. The literature-reported fat T_1 value is shown as a solid gray line.